

# THREE ASTROMETRIC MISSION OPTIONS AND A PHOTOMETRIC SYSTEM<sup>1</sup>

E. Høg

Copenhagen University Observatory  
Østervoldgade 3, 1350 Copenhagen K, Denmark  
Electronic mail: erik@astro.ku.dk

## ABSTRACT

Three options of future space astrometry missions are discussed, including combinations of interferometric and direct, incoherent image detection techniques. The great astrometric advantage of off-axis telescopes is quantified. Astrometric and photometric performances are given as function of magnitude. The proposed eight-band photometric system, called *Stromvil+I*, consists of four Strömgren bands, three Vilnius bands and the Cousins infrared band, and it is suited for determination of accurate stellar parameters and interstellar reddening. – Two options in the 10  $\mu\text{as}$  accuracy class at  $V = 14$  mag are discussed. A third smaller option in the 100  $\mu\text{as}$  class is also given, using a 30 cm beam combiner and only direct image detection. It seems that the scientific performance with respect to accuracy and limiting magnitude of astrometry and photometry is superior for the direct image detection technique for field stars, stars in clusters and wide double stars. Interferometry excels in angular resolution of narrow double stars.

Keywords: space astrometry; ROEMER; GAIA; photometry.

## 1. INTRODUCTION

Three efficient options of scanning astrometric satellites are presented. The great astrometric advantage of off-axis telescopes in a satellite is pointed out. The discussion is based on the use of CCDs in drift scan mode, also called Time Delay Integration, TDI.

Options using incoherent, direct image detection in the ROEMER proposals (Høg 1993, Lindegren *et al.* 1993, Høg & Lindegren (1994), Høg 1994, Høg 1995) are combined with the interferometric telescopes for GAIA described by Lindegren & Perryman (1994), hereafter referred as LP. This results in two very robust mission designs capable of achieving a high accuracy for global astrometry and a high angular resolution.

The option R80.G, Fig. 1, contains a ROEMER-section with two telescopes of 80 cm aperture scanning the same

great circle. These two fields of view are supplemented with an interferometric GAIA-section with one field of view, scanning the same great circle. The letters R and G are used as abbreviations for ROEMER and GAIA. With these three directions of view a very rigid great circle solution will be obtained, cf. Makarov *et al.* (1995). Furthermore, the interferometric section will obtain a much higher angular resolution of double and multiple stars than an R-section. The whole system is simple and robust since high quality results would be obtained even if one of the three directions of view would not perform as specified. It is more robust than the proposed GAIA with three interferometric sections scanning the same great circle because a direct imaging telescope is simpler than an interferometric.

The astrometric errors of the R80-section are less than 10  $\mu\text{as}$  at  $V = 14$  mag from a 5 years mission. They are supplemented with precision photometry in eight bands, identical for the two 80 cm telescopes. The proposed photometric system, called *Stromvil+I*, consists of four Strömgren bands, three Vilnius bands and the Cousins infrared band, and it is suited for determination of accurate stellar parameters and interstellar reddening, as discussed by Straizys & Høg (1995).

The second option R55.G, Fig. 2, is very similar to the previous one, except that the ROEMER section has telescopes of apertures 55 cm, and that their optical axes are folded differently, namely so that they lie entirely in one plane, that of the great circle.

A third smaller mission option, Fig. 4, in the 100  $\mu\text{as}$  accuracy class is given, using a 30 cm beam combiner and only direct image detection.

## 2. OFF-AXIS TELESCOPE

The effect of five design parameters of a direct imaging telescope for the performance of an astrometric mission has been studied: Telescope aperture  $D$ , focal length  $F$ , central linear obscuration  $\epsilon$  of the telescope, the area  $A_{\text{astrom}}$  [steradian] of the focal plane covered with CCDs for astrometry, and the width  $w$  [ $\mu\text{m}$ ] of the pixels along scan.

<sup>1</sup>A contribution to *Future Possibilities for Astrometry in Space*, a workshop at RGO, Cambridge, England, 19-21 June 1995

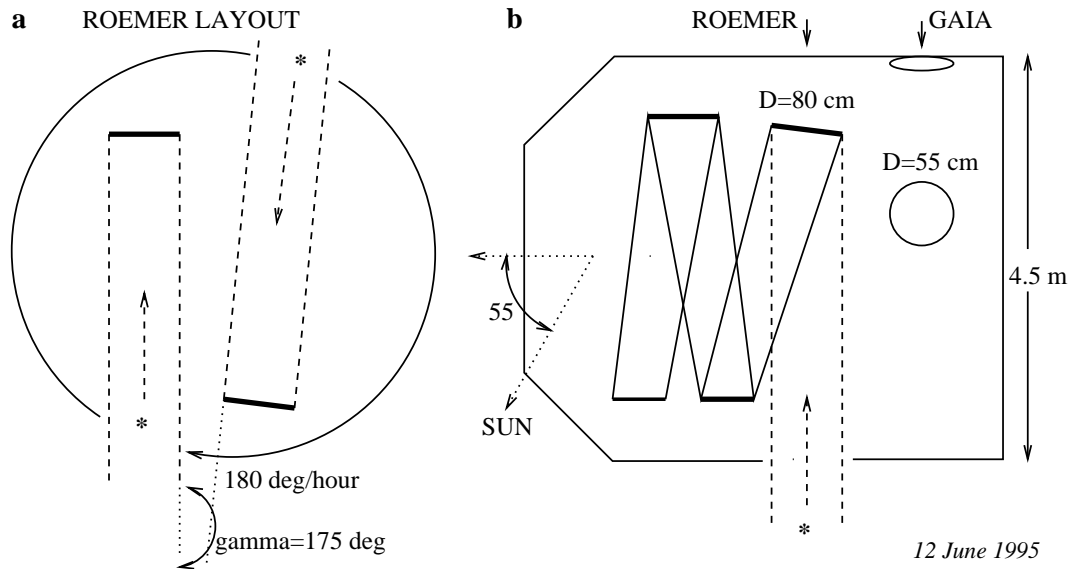


Figure 1: Optical layout of the option R80.G. (a) R-section: Two telescopes with  $D = 80 \text{ cm}$  are scanning the same great circle. Their respective optical axes are folded in planes perpendicular to the great circle, (b) one of the R-telescopes and the two apertures of the G-telescope with  $D = 55 \text{ cm}$  are shown.

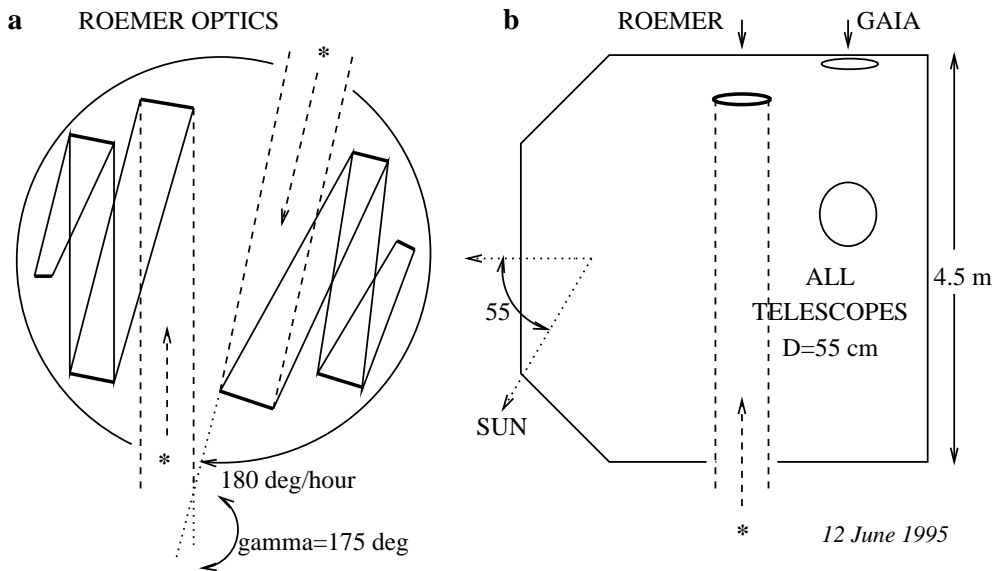


Figure 2: Optical layout of the option R55.G. (a) R-section: Two identical off-axis telescopes with  $D = 55 \text{ cm}$  pointed an angle  $\gamma = 175 \text{ deg}$  apart are scanning the same great circle. Their respective optical axes are folded in a plane perpendicular to the spin axis, (b) the satellite contains also an interferometric GAIA section consisting of two off-axis telescopes optically identical to those of the R-section.

The standard error  $\sigma_{\text{astrom}}$  of an astrometric parameter for a star is a function of these five parameters:

$$\sigma_{\text{astrom}} = C_{\text{astrom}} D^{-2} A_{\text{astrom}}^{-0.5} (1 - \epsilon^2)^{-0.5} (1 + 1.8 \epsilon^2)(1 + 2.0 wD/F) \quad (1)$$

where the constant depends on other than the five parameters, such as the magnitude and colour of the star, the quantum efficiency  $QE$ , of the detector, length of the mission, position of the star in the sky, etc. The formula takes only photon noise of the star light into account, as described by Høg (Annex B, p. 28 of Lindegren *et al.* 1993). The high power (2) of  $D$  is due to the number of photons collected by the aperture and to the angular resolving power of the telescope. It appears that the telescope must be as large as resources permit. The angular field free of optical aberrations must be as large as possible; we shall assume 1.6 degrees diameter in the following, the same as LP, but an optimization requires optical studies of the proper three mirror systems.

The first bracket in Eq. (1) is due to the loss of light from the central obscuration. The coefficients in the two last brackets have been derived from calculations of the astrometric performance and this part of the formula gives the correct dependence within 10 percent if  $\epsilon \leq 0.5$  and  $0.1 < wD/F [\mu\text{m}] < 1.0$ . For simplicity of calculation monochromatic light of  $\lambda 600 \text{ nm}$  was assumed instead of the true spectral distribution of star light. The factor due to a central obscuration is in total 1.67 for  $\epsilon = 0.5$ , and such an obscuration is required to obtain a large field in a centred optical system, as for instance the ROEMER+ system proposed by Høg (1995). Another disadvantage of a centred system derives from the large  $D/F$  ratio  $\simeq 0.10$  required because of the large field, and this  $D/F$  ratio enters into the last bracket of the equation. Since  $w \simeq 6 \mu\text{m}$  is the smallest pixel width that can be manufactured today the last bracket gives a factor 2.20, thus the three brackets give altogether a factor  $1.67 \cdot 2.20 = 3.67$  for a centred system.

An off-axis system has, however, no central obscuration, and with a  $D/F = 0.05$  we obtain a factor of only 1.60 from the three brackets in the equation. Therefore an off-axis telescope system is much to be preferred, for instance the three-mirror system proposed for GAIA. The first proposal for a ROEMER mission (Høg 1993) contained an off-axis system, but this was replaced by centred systems in the later ROEMER proposals listed above because Dr. R.N. Wilson had drawn my attention to the great difficulties of off-axis telescopes: They are difficult to manufacture with superb accuracy, difficult to adjust and difficult to keep adjusted. But the advantage in theoretical performance is so great that these difficulties should be acceptable for an astrometric space mission. Thus, for all the following mission options we assume  $D/F = 0.05$ ,  $w = 6 \mu\text{m}$ ,  $\epsilon = 0.0$  and a field diameter of 1.6 degrees.

The star image formed by an off-axis telescope will be elongated along the plane of the folded axes if the optical aberrations are significant. The better astrometric accuracy will be obtained if the short axis of the elongated image goes along the scan direction; in fact the elongation will not disturb this accuracy at all. This gives an advantage for the two following options with  $D = 80$  and  $30 \text{ cm}$  since they are folded perpendicular to the scan direction.

The standard error  $\sigma_{\text{phot}}$ , of a photometric quantity is

given by

$$\sigma_{\text{phot}} = C_{\text{phot}} D^{-1} A_{\text{phot}}^{-0.5} (1 - \epsilon^2)^{-0.5} \quad (2)$$

observed by an area  $A_{\text{phot}}$  [steradian] of CCDs.

The Eqs. (1) and (2) are valid in cases where the background is negligible compared with star light, which is true for all but the faintest stars. Note, however, that the following Tables take background, readnoise etc. into account, see Sect. 4. The equations are valid if all detected photons are used optimally in the estimation.

The optical-mechanical system should satisfy the following requirements. The optical surfaces and their adjustment must be of diffraction limited quality for the R- and G-sections. The requirement is most stringent for the G-section in order to ensure optimal fringe visibility, whereas a slight widening of the diffraction image along scan will only affect the astrometric error of the incoherent R-section as an increase of the pixel width  $w$  in Eq. (1). Furthermore, the two beams of the interferometric G-section should have a path length difference less than  $\simeq 1 \mu\text{m}$  at the center of a star image, and the two diffraction images should coincide within a fraction of the diameter, i.e., within 10 mas.

### 3. INTERFEROMETRY AND DIRECT IMAGING

Combinations of interferometric and two different sizes of direct imaging telescopes are considered, as outlined in Sect. 1. This results in performances in the  $10 \mu\text{as}$  accuracy class. The calculations are realistic with respect to photon noise, taking into account for instance the diffracted star image, a realistic background from the sky, scattered light, readnoise and quantum efficiency. The calculations assume that the effects of e.g., parasitic stars, attitude jitter, optical aberrations and systematics are negligible.

#### 3.1. Mission with 80 cm Telescopes – R80.G

The proposed satellite is shown in Fig. 1. The R-section with two reflecting telescopes of  $D = 80 \text{ cm}$  observe two fields on the sky separated by the basic angle  $\gamma$  of about 148 degrees. This angle must be monitored by suitable metrology of mirror angles and positions during short time scales. On longer time scales than the 2 hours spin period the angle will be calibrated by means of the star observations. The focal plane arrangement of CCDs is similar to that of Fig. 3, but enlarged to a scale of  $12.4 \text{ arcsec/mm}$ . The  $F/D$  ratio is 0.05 and the pixel width remains  $6 \mu\text{m}$  for manufacturing reasons.

An interferometric G-section observes a third field on the same great circle as the R-section. The direction of view of the G-section is monitored and calibrated relative to the two directions of the R-section.

The astrometric and photometric performances of the R-section are given in Table 1. It appears that a five year mission would give errors of less than  $10 \mu\text{as}$  at  $V = 14 \text{ mag}$  and photometric errors less than 0.010 mag for most bands at  $V = 17 \text{ mag}$ .

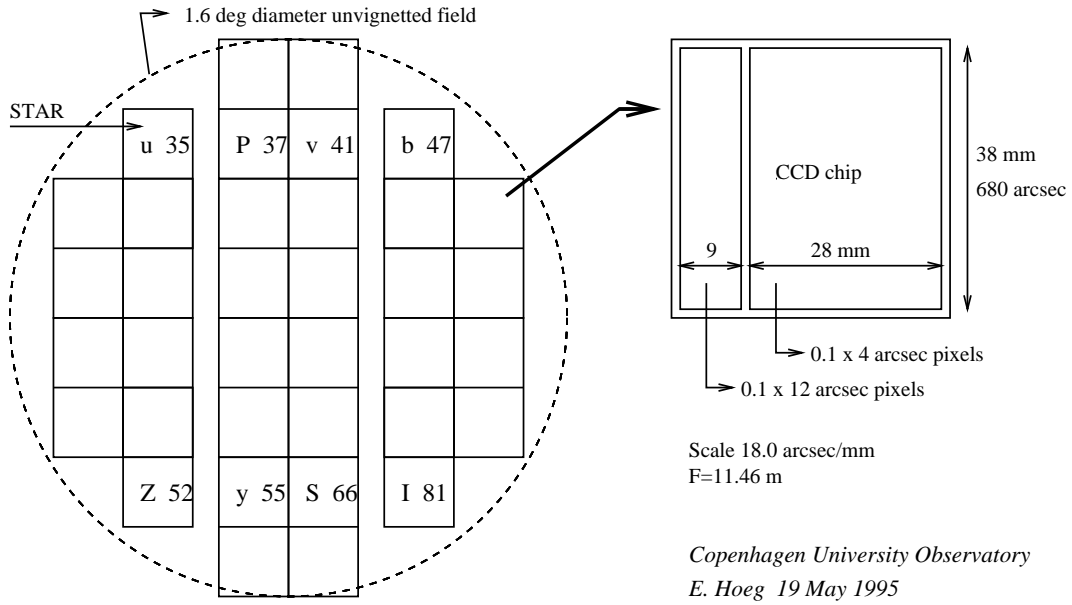


Figure 3: Focal plane arrangement of CCDs. The photometric bands are designated by one letter, or the rounded central wavelength: [nm/10]. No designation in a square area means a wide band  $W$ , namely the whole spectral range of the CCD. The scale of 18.0 arcsec/mm corresponds to the R55-section with a telescope of  $D = 55$  cm and  $F = 11.46$  m.

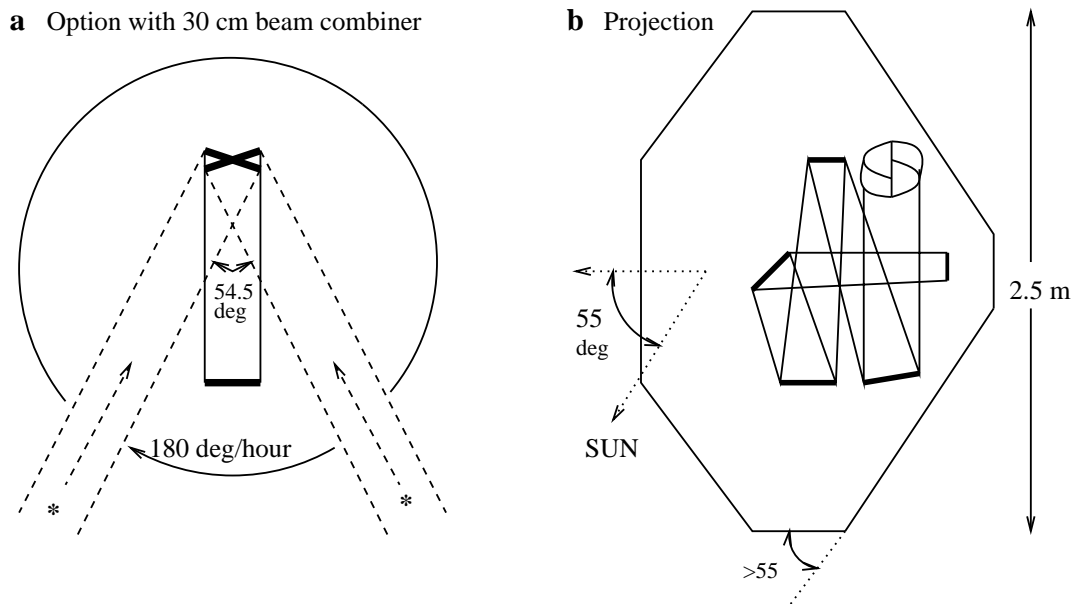


Figure 4: Optical system R30, with a  $D = 30$  cm Hipparcos-type beam combiner and  $F = 6$  m which may be placed inside a cylinder of about 2.5 m diameter. A three-mirror reflecting telescope and a flat 45-degree mirror produce a focus at the cold side of the satellite.

### 3.2. Mission with 55 cm Telescopes – R55.G

The satellite in Fig. 2 contains an R-section with two telescopes of  $D = 55$  cm having all optical axes folded in one plane, the plane of the scanned great circle. It is simpler to monitor the angles and positions of the mirrors in such a two-dimensional arrangement than in the three-dimensional R80-section. The penalty for this constructive advantage is the smaller aperture of 55 cm that can be accommodated within the 4.5 m diameter cylinder of an Ariane 5 launcher. The satellites shown in Figs. 1 and 2 may be provided with solar power and a sunshield as described by Høg (1995b).

The astrometric and photometric performances of the R-section may be obtained from Table 1 by multiplication of the astrometric errors with a factor 2.2 and the photometric errors with a factor 1.5.

### 3.3. Choice of Basic Angle

A basic angle  $\gamma = 175$  deg is shown in Figs. 1 and 2. This angle still provides a high rigidity in the great circle reduction, according to Fig. 2.1 in Perryman & Hassan (1989), and it would give an optimal accuracy for parallaxes. The angle is so close to 180 deg that an accurate determination of the position of the z-axis, the body axis along the spin axis, is not possible. But a high accuracy is not really required for the purpose of projecting the field measurements on a reference great circle. Furthermore, an accurate determination of the z-axis position is possible when the observations in the third direction of view by the G-section are taken into account.

### 3.4. Combinations – Conclusions

The astrometric performance of various combinations are given in Table 2. The parallax errors due to photon noise are given in the first two lines (3Gcoh and 3Ginc) for GAIA consisting of three sections, and are taken from columns #2 in the Tables 3 and 4 of LP. The columns #4 and 5 in LP-Table 3 show the errors for direct fringe detection which is not considered by LP to be a realistic option for the present. It has been verified that the errors given in the line 3Ginc are reproduced reasonably well by our calculations; we obtain 20 percent smaller errors, see Straizys & Høg (1995). One GAIA-section (line #3) gives  $\sqrt{3}$  times larger errors than the combination of 3Gcoh and 3Ginc. The errors given in the following lines for the two ROEMER-sections are combined by statistical weighting with the errors for one GAIA-section, resulting finally in the expected errors for the mission options R80.G and R55.G in the last two lines of Table 2.

The two ROEMER-GAIA options give errors less than  $10 \mu\text{as}$  at  $V = 14$  mag, similar to GAIA with three interferometric sections. The R80.G is the best of all proposed options. The given errors take only photon noise into account, not errors due to, for instance, non-ideal adjustment of optical elements. Ideal performance can most probably be obtained for the technically simple ROEMER sections. Even if the ideal performance of the more complicated GAIA sections cannot be guaranteed, the combination with the proposed ROEMER sections would produce a satellite with ideal performance for global astrometry and give an opportunity to achieve a high resolution of a large number of non-single stars by interferometry.

The scientific justification for the mission should be discussed for three categories of stars: field stars, stars in clusters, narrow double stars.

1. Global astrometry of field stars. An R80-section is equivalent to GAIA with three sections for stars brighter than  $V \simeq 16$ , but superior to GAIA for fainter stars, cf. Table 2.
2. Global astrometry in clusters or dense fields of stars. Similar to (1), but the limit will be brighter than  $V = 16$ , depending on the star density. Stars with separations  $> 1$  arcsec can be separated by an R-section from scans in many directions. With interferometric measurement, however, below 10 arcsec separation the stars will disturb each other too much because of the large instantaneous field of view of about  $27 \times 14$  arcsec<sup>2</sup>, according to LP-Fig. 7.
3. Double star in an uncrowded field. The components may, according to LP-Sect. 2.2, be separated by interferometry even as close as  $\simeq 1 - 2$  mas, the fringe spacing being  $\simeq 54$  mas. The incoherent imaging can perhaps only resolve components with separations of  $\simeq 50$  mas.

It appears that the scientific performance of the proposed interferometric techniques is superior at double stars with separations  $< 50$  mas. The direct, incoherent image detection seems to be superior for astrometry and photometry of single stars, stars in clusters and for double stars with wider separations.

## 4. OPTION WITH BEAM COMBINER

A satellite, R30, with  $D = 30$  cm beam combiner is shown in Fig. 4. A reflective beam combiner of the type used in HIPPARCOS has been shown to be stable enough for a mission aiming at  $100 \mu\text{as}$  accuracy. Metrology could be used to monitor the angle of the beam combiner, if required. A telescope with  $F = 20 \times D = 6$  m and a focal plane arrangement similar to Fig. 3 is assumed.

The resulting astrometric and photometric performance for a 2.5 year mission is given in Table 3. The parallax errors are about  $100 \mu\text{as}$  at  $V = 13$  mag. At the same magnitude the photometric errors are about 0.010 mag for an intermediate band.

The effect of changing some assumptions is of interest. If the pixel width is  $w = 9 \mu\text{m}$  instead of  $6 \mu\text{m}$  the astrometric errors in Table 3 should be multiplied by a factor 1.9/1.6, according to Eq. (1). The errors should be multiplied by  $\sqrt{0.78/0.3} = 1.6$  if the maximum QE is 0.3, as expected from frontside CCDs, altogether a factor 1.9. This means proper motion errors of  $\simeq 100 \mu\text{as}$  at  $V = 10$  from a 2.5 year mission. A readnoise of 1.5 e-per CCD crossing was assumed, in accordance with the time available to read the relevant charges if an input catalogue is used. A pessimistic readnoise of 5 e-only affects the astrometry of the faintest stars, for instance the errors increase by 10 percent at  $V = 16$  in Table 3, and at  $V = 20$  in Table 1. But the intermediate band photometry is more disturbed; the errors in the  $y$ -band increase by 50 percent at  $V = 15$  in Table 3, and at  $V = 18$  in Table 1.

Table 1: For an R80-section, two telescopes of 80 cm aperture, 5 year mission: Predicted standard errors due to *photon noise* in astrometry and photometry for a G0-star. The effects of e.g., background, readnoise and undersampling are included. Filter- and CCD characteristics are given at the bottom, and line #3 contains the rounded central wavelength [nm/10] for each band. A minus (-) at bright stars means non-linear response of the CCD, i.e.  $> 3000e^- \mu\text{m}^{-2}$  in a pixel. At faint stars a minus means a signal-to-noise ratio  $\leq 2.0$  on a single CCD crossing. Unit: mas = milliarcsec.

V mag	Astrometry		W	Photometry [millimagnitude]							
	par. mas	p.m. mas/year		u 35	P 37	v 41	b 47	Z 52	y 55	S 66	I 81
2	0.001	0.001	-	0.0	0.0	0.0	-	-	-	-	-
4	0.001	0.001	-	0.1	0.1	0.1	0.0	0.0	0.0	0.0	0.0
6	0.001	0.001	-	0.1	0.1	0.1	0.1	0.0	0.0	0.1	0.0
8	0.001	0.001	0.0	0.4	0.3	0.2	0.1	0.1	0.1	0.1	0.0
10	0.001	0.001	0.0	0.9	0.8	0.5	0.4	0.3	0.3	0.3	0.1
12	0.003	0.002	0.0	2.4	2.0	1.2	0.9	0.8	0.7	0.8	0.3
14	0.008	0.005	0.1	6.0	5.2	3.0	2.2	1.9	1.9	2.1	0.8
16	0.021	0.012	0.2	16.1	13.7	7.6	5.7	4.9	4.7	5.4	2.0
18	0.057	0.034	0.5	60.3	49.3	21.7	15.7	13.4	12.9	14.7	5.3
20	0.195	0.114	1.4	-	-	-	61.3	50.9	48.4	56.7	16.5
22	1.015	0.593	6.5	-	-	-	-	-	-	-	-
Central wavelength [nm]	-	-	-	350	374	411	467	516	547	656	812
Filter FWHM [nm]	-	-	-	30	26	19	18	21	23	20	166
Peak transmission	-	-	-	0.40	0.42	0.60	0.70	0.80	0.80	0.80	0.90
QE of CCD	-	-	-	0.68	0.72	0.74	0.78	0.77	0.76	0.73	0.62

Table 2: Global astrometric performance as function of magnitude of some instrument combinations for 5 year missions, cf. Sect. 3.4. Note e.g., that the performances are similar for a GAIA mission with three instrument sections (3Gcoh+3Ginc) and an R55.G mission with two sections.

Instrument combination	Standard error of parallax [ $\mu\text{as}$ ]						
	at V = 10	12	14	16	18	20	22
<b>3Gcoh, GAIA coherent</b>	2	3	6	20	-	-	-
<b>3Ginc, GAIA incoherent</b>	3	8	20	50	140	500	-
One G-section	4	5	10	35	240	850	-
R80-section	1	3	8	21	57	195	1020
R55-section	3	7	18	46	127	466	-
R80.G	1	3	6	18	55	190	1020
<b>R55.G</b>	2	4	9	28	112	409	-

Table 3: For an R30-satellite, beam combiner of 30 cm aperture, 2.5 year mission: Predicted standard errors due to *photon noise* in astrometry and photometry for a G0-star. See Table 1 for further explanations. Unit: mas = milliarcsec.

V mag	Astrometry		W	Photometry [millimagnitude]							
	par. mas	p.m. mas/year		u 35	P 37	v 41	b 47	Z 52	y 55	S 66	I 81
2	0.008	0.009	-	0.2	0.2	0.2	0.1	0.1	0.1	0.1	-
4	0.009	0.011	-	0.5	0.4	0.2	0.2	0.1	0.1	0.2	0.1
6	0.008	0.009	0.0	1.1	1.0	0.6	0.4	0.4	0.4	0.4	0.2
8	0.011	0.013	0.0	2.9	2.5	1.4	1.1	0.9	0.9	1.0	0.4
10	0.027	0.032	0.1	7.3	6.3	3.6	2.7	2.4	2.3	2.6	1.0
12	0.068	0.080	0.2	18.7	16.1	9.2	6.9	6.0	5.7	6.5	2.4
14	0.174	0.204	0.5	53.5	44.9	24.0	17.8	15.4	14.7	16.7	6.2
16	0.473	0.552	1.4	-	-	83.1	51.5	43.5	41.5	47.9	16.4
18	1.603	1.872	4.4	-	-	-	-	-	-	-	52.2
Central wavelength [nm]	-	-	-	350	374	411	467	516	547	656	812
Filter FWHM [nm]	-	-	-	30	26	19	18	21	23	20	166
Peak transmission	-	-	-	0.40	0.42	0.60	0.70	0.80	0.80	0.80	0.90
QE of CCD	-	-	-	0.68	0.72	0.74	0.78	0.77	0.76	0.73	0.62

## ACKNOWLEDGEMENTS

This work was supported by the Danish Space Board. The author is grateful for useful discussions and for comments to a previous version of this paper by Drs C. Fabricius and V.V. Makarov. I am also indebted to Drs. L. Lindegren, F. van Leeuwen, M. Shao and V. Straizys for inspiring comments on the subject.

## REFERENCES

- Høg E. 1993, Astrometry and photometry of 400 million stars brighter than 18 mag, in: *I.I. Mueller and B. Kotaczek (eds.) Developments in Astrometry and Their Impact on Astrophysics and Geodynamics, IAU Symp. No. 156*, 37.
- Høg E., 1994, A new era of global astrometry and photometry from space and from ground, contribution at the 'G. Colombo' Memorial Conference: *Ideas for Space Research after the year 2000*, Padova, 18,19 February 1994.
- Høg E. 1995, A new era of global astrometry. II: A 10 microarcsecond mission, in E. Høg and P.K. Seidelmann (eds.) *Astronomical and Astrophysical Objectives of Sub-milliarcsecond Optical Astrometry*, IAU Symposium No. 166, The Hague August 1994, Kluwer, Dordrecht.
- Høg E. 1995b, Astrometric Satellite with Sunshield, submitted to: *Future Possibilities for Astrometry in Space*, by M.A.C. Perryman and F. van Leeuwen (eds.), a workshop at RGO, Cambridge, England, 19-21 June 1995, ESA Publications Division, ESTEC
- Høg, E., Lindegren, L. 1994, ROEMER satellite project: The first high-accuracy survey of faint stars. In: *Galactic and Solar System Optical Astrometry*, by L. V. Morrison & G. Gilmore (Eds.), 246-252, Cambridge University Press.
- Lindegren L. (ed.) 1993, *ROEMER - Proposal for the Third Medium Size ESA Mission (M3)*, Lund.
- Lindegren L., Perryman M.A.C. 1994, GAIA - Global Astrometric Interferometer for Astrophysics, in *Supplementary Information Submitted to the Horizon 2000+ Survey Committee*, 52pp.
- Makarov V.V., Høg E., Lindegren L. 1995, Random errors of star abscissae in the ROEMER space astrometry project, submitted for publication in *Experimental Astronomy*
- Perryman M.A.C., Hassan H. 1989, *The Hipparcos mission*, Vol. 1, *The Hipparcos Satellite*. ESA Publications Division, ESA SP-1111.
- Straizys V., Høg E. 1995, An optimum 8-colour photometric system for a survey satellite, submitted to: *Future Possibilities for Astrometry in Space*, by M.A.C. Perryman and F. van Leeuwen (eds.), a workshop at RGO, Cambridge, England, 19-21 June 1995, ESA Publications Division, ESTEC